Supporting Information

Formation of CdTe core and CdTe@ZnTe core-shell Quantum Dots via Hydrothermal Approach using Dual Capping Agents: Deciphering the Food Dye Sensing and Protein Binding Applications

Mahabul Haque[a], Jintu Chutia[a], Amarjyoti Mondal[a], Sana Quraishi[a], Kalpana Kumari[b] Erica W M Marboh[c], Kripamoy Aguan[c] and Atanu Singha Roy[a,*]

[a]Department of Chemical and Biological Sciences, National Institute of Technology Meghalaya, Shillong, 793003, India

[b]Department of Bioscience and Bioengineering, Indian Institute of Technology, Guwahati, 781039, India

[c]Department of Biotechnology & Bioinformatics, North-Eastern Hill University, Shillong 793022, India

***Corresponding Author:** Atanu Singha Roy

Tel.: +91 364 2501294

Fax: +91 364 2501113

Email: singharoyatanu@gmail.com; asroy86@nitm.ac.in

1. Experimental procedures

1.1. Sensing studies

Sensing studies were conducted using Agilent Cary Eclipse fluorimeter based on the fluorescence probe. The excitation wavelength (λ_{ex}=370 nm) was selected for the fluorescence probes CdTe-PVP and CdTe@ZnTe-PVP QDs via a monochromator keeping the fixed excitation/emission slit width 10/5 nm (λ_{em}=400-650 nm). 0-50 µM food dyes (carmoisine, ponceau and tartrazine) were added to the respective fluorescence probes in a dose-dependent manner, and collected the fluorescence quenching spectra were at intervals of 2 minutes. All the experiments were performed in phosphate buffer (PB) of pH 8.0 and in triplicates.

Sensing of food dyes in real samples

Real samples (Levosalbutamol Sulphate, Ambroxol Hydrochloride and Guaiphenesin Syrup: Tartrazine, Salbutamol Sulphate Syrap: Carmoisine and Soft drinks) were purchased from a local medical shop and local store. The samples were centrifuged at 12000 rpm for 10 minutes and 100 µL of each supernatant solution was diluted to 3000 µL using PB. The diluted supernatant solutions were then subjected for analysis in the absence and presence of spike concentrations of respective food dyes.

1.2. Fluorescence measurements of HSA-QDs interactions

Fluoromax-4 Jobin Yvon fluorometer with a Newport temperature regulator (Model 350 B, California, USA was utilized to investigate the HSA and synthesized QDs interactions based on the intrinsic fluorescence quenching of HSA. Using a high-quality quartz cuvette 3 µM HSA solution was titrated with respective CdTe-PVP and CdTe@ZnTe-PVP QDs (0-19.7 µM) upon excitation of 295 nm and keeping the fixed slit width 5/5 nm (λ_{em}=305-450 nm) at varying temperatures (288, 298 and 308 K). HSA solutions were incubated for 15 min prior to titration with the respective synthesized QDs. All the interaction studies were conducted *in vitro* conditions and at a physiological pH of 7.4. Each experiment was performed in triplicates and

necessary blank scans were carried out for ligands (synthesized QDs). The fluorescence decay profiles were corrected with inner filter effect (IFE)[1] before being analyzed the spectra using following equation (**eqn. S1**)

$$F_{cor} = F_{obs} \times 10^{\frac{(A_{ex.} + A_{em.})}{2}} \quad \text{S1}$$

Where $A_{em.}$ and $A_{ex.}$ signifies the absorbances of the respective synthesized CdTe-PVP and CdTe@ZnTe-PVP QDs, respectively, at the emission (346 nm) and excitation wavelength (295 nm) of HSA. F_{obs} and F_{cor} represents the observed and corrected fluorescence intensities, respectively.

To elucidate the microenviron alteration around the protein fluorophore residues (tryptophan: Trp and tyrosine: Tyr) upon interaction with QDs, the synchronous fluorescence spectra of HSA (3 μM) were recorded in the presence of respective synthesized QDs (0-19.7 μM) by setting the wavelength difference Δλ=60 nm (for Trp) and Δλ=15 nm (for Tyr).[2]

The red edge excitation shift (REES) effect was investigated by exciting of HSA (3 μM) and 1:2 HSA-QDs (CdTe-PVP/CdTe@ZnTe-PVP) complexes at 295 and 305 nm, respectively, keeping the fixed slit width 5/5 nm.

The fluorescence anisotropy measurement was carried out in Agilent Cary Eclipse fluorescence instruments by setting the excitation and emission slit width 5/5 nm. The excitation and emission wavelengths for CdTe-PVP QDs were 370 and 462 nm, and for CdTe@ZnTe-PVP QDs were 370 and 462 nm, respectively. 20 μM of each QDs solution was titrated with HSA (0-100 μM) at a constant temperature of 298 K.

1.3. Excited state lifetime analysis

The fluorescence lifetime measurements were carried out based on the Time-Correlated Single Photon Counting (TCSPC) instrument (LifeSpec II model: FSP 920, Edinburg Instrument, UK). HSA and their complexes with CdTe-PVP and CdTe@ZnTe-PVP QDs were stimulated

with 295 nm LED source and the QDs and their complexes with food dyes (carmoisine, ponceau 4R, and tartrazine) were stimulated using 375 nm laser source. All the lifetime decay profiles were recorded at a magic angle of 54.7°. A coffee whitener was utilized to calculate the instrument response function (IRF). The decay traces were analyzed by non-linear least square method based on Lavenberg-Marquardt techniques[3] and with reference to IRF. The accuracy of the graphical fits was estimated by visual comparison of the residual of the fitted function with the Durbin-Watson parameter and χ^2 value. **Eqn. S2** states the sum of time-dependent decay profiles.

$$F = \sum_i \alpha_i e^{-\frac{t}{\tau_i}} \quad \text{(S2)}$$

Where α_i and τ_i symbolizes the amplitude and lifetime of ith element. The average lifetime (τ_{avg}) was computed by employing the following equation (**eqn. S3**)

$$\tau_{avg} = \frac{\sum_i \alpha_i \tau_i^2}{\sum_i \alpha_i \tau_i} \quad \text{(S3)}$$

1.4. Absorption studies

Using PerkinElmer Lambda 35 spectrophotometer, the absorption spectra of HSA and HSA-QDs complexes were recorded. Using a pair of quartz cuvette (path length 1 cm), 10 μM HSA and 1:1 QDs complexes were scanned within the range 250-400 nm in a 20 mM phosphate buffer of pH 7.4.

1.5. Circular dichroism (CD) measurements

Far UV CD of HSA (3 μM) and 1:2 QDs complex were carried out using JASCO-J1500 CD instrument in the scanning range 190-240 nm (scan rate 100 nm/minute) with the help of a quartz cuvette of path length 0.1 cm. For collecting the CD data, 1 nm bandwidth and 4 s

response time were used. Utilizing an online server, DICHROWEB,[4], the percentage of secondary structural components of HSA and the complexes with respective CdTe-PVP/CdTe@ZnTe-PVP QDs have been determined.

1.6. Determination of Quantum yields (QY)

The comparison method[5,6] the QY of the synthesized CdTe-PVP and CdTe@ZnTe-PVP QDs were estimated based following equation (**Eq S4**) using anthracene as a standard refence.[5]

$$\Phi_{QDs} = \Phi_{Anthra.} \times \frac{\mu_{QDs}}{\mu_{Anthra.}} \times \left(\frac{\eta_{QDs}}{\eta_{Anthr.}}\right)^2 \quad \text{(S4)}$$

Where ϕ_{QDs} and $\phi_{\text{Anthra.}}$ represent the QY of respective QDs (CdTe-PVP and CdTe@ZnTe-PVP QDs) and anthracene, respectively. μ_{QDs} and $\mu_{Anthra.}$ signifies the slopes of the integrated fluorescence intensity vs. absorbance plot. η_{QDs} and $\eta_{Anthr.}$ are the refractive indices of the medium (1.33 for water and 1.36 for ethanol as the solvent). The concentrations of the respective QDs and anthracene were set in such a way that absorbance of the solution lies in between 0.01 and 0.1 a. u. The experiments were performed in ethanol and water for anthracene and respective QDs, respectively, by fixing the excitation wavelength (λ_{ex}) 370 nm and emission region 390-600 nm for fluorescence measurement.

1.7. Förster resonance energy transfer (FRET) estimation

The energy transfer efficiency in a donor-acceptor is given by the following equation:[7–9]

$$E = \frac{1}{1 + (\frac{r}{R_0})^6} \quad \text{(S5)}$$

where r is the distance of the donor-acceptor pair, and R_0 is the critical distance at which the efficiency of energy transfer is 50%. The value of R_0 is calculated using the following equation:[7]

$$R_0 = [\frac{9000\phi_0(ln10)\kappa^2 J(\lambda)}{128\pi^5 N^4 N_A}]^{1/6}$$

(S6)

where ϕ_0 is the fluorescence quantum yield of the donor (QDs), κ^2 is the donor-to-acceptor dipole orientation factor (2/3), $J(\lambda)$ is the spectral overlap integral, N is the refractive index of the medium and N_A represents the Avogadro's number.

The spectral overlap integral is estimated using the following equation:

$$J(\lambda) = \int F_D(\lambda)\varepsilon_A(\lambda)\lambda^4 d\lambda \quad \text{(S7)}$$

Where F_D is the normalized fluorescence spectrum of the donor, λ is the wavelength, and ε_A is the molar extinction coefficient of the acceptor molecule.

The FRET efficiency can be measured experimentally and is commonly defined as[7]

$$E = 1 - \frac{F_{DA}}{F_D} \quad \text{(S7)}$$

where F_{DA} is the integrated fluorescence intensity of the donor in the presence of the acceptor (A) and F_D is the integrated fluorescence intensity of the donor alone.

1.8. Cell cytotoxicity studies: MTT assay

The toxicity level of synthesized CdTe-PVP and CdTe@ZnTe-PVP QDs were investigated against rat skeletal muscle cell line L6 (primary cell lines) via MTT assay. It is a colorimetric assay, which depends on the quantitative assessment of metabolically active cells cleaving the tetrazolium dye 3-[4, 5-dimethylthiazol-2-yl]-2, 5-diphenyl tetrazolium bromide (MTT) into insoluble purple formazan crystals. The intensity of the purple color is directly proportional to the number of live cells and can be estimated by applying spectrophotometry. Freshly extracted L6 cells from a culture flask were diluted to a concentration of 1×10^3 cells/mL using Gibco, ThermoFishers Advance MEM culture media and seeded in 96-well microtiter plates (in triplicate) with 100 µL of L6 cell suspension. The plates were incubated for 24 h at 37 °C using

a 5% CO_2 incubator, and after 24 h incubation, the medium was withdrawn and replaced with 100 µL of fresh DMEM (Low Glucose without Phenol, Himedia) containing varying concentrations of respective QDs (0, 0.5, 1, 2.5, 5 and 10 µg/mL). The QDs-treated cells were left for another incubation period of 24 h. The plate was then taken off from the incubator, 10 µL of MTT reagent was added to each well, and the plate was wrapped in aluminium foil to prevent light exposure before being placed back in the incubator for another 4 h. Finally, 100 µL of the solubilization was poured solution to each well, and the plates were shaken for thirty minutes to allow for complete disintegration of the formazan crystal. The absorbance at 570 nm was recorded using a 96-well plate reader (Synergy H1 Hybrid reader, BioTek), and the % cell viability was estimated using the following relationship (**Eq S8**).

$$\%\ Cell\ viability = \frac{Absorbance\ of\ the\ QDs - treated\ cells}{Absorbance\ of\ the\ control} \quad \text{(S8)}$$

2. Results

Table S1: Comparison of LOD values for the detection of food dyes, carmoisine, ponceau 4R and tartrazine using the proposed sensing probes with the reported literatures

Sensing probe	Sensing molecule	Methods	LOD values	Concentration range	References
Ni-Co LDH nanosheet	Carmoisine	Electrochemical sensing	0.09 µM	0.3-125 µM	[10]
Fe3O4 (GO-Fe3O4) nanocomposite		Electrochemical sensing	0.02 µM	0.1-170 µM	[11]
ZnO-Graphite electrode		Cyclic voltammetry	0.02 µM	0.08-180 µM	[12]
CdTe-PVP		Fluorescence	0.097±0.006 µM	0-50 µM	Present work
CdTe@ZnTe-PVP		Fluorescence	0.079±0.001 µM	0-50 µM	Present work
Graphene QDs	Ponceau 4R	Fluorescence	2.57 µg/mL	5-150 µg/mL	[13]
Carbon QDs		Fluorescence	40 nM	60-6000 nM	[14]
CdTe-PVP		Fluorescence	0.147±0.001 µM	0-50 µM	Present work
CdTe@ZnTe-PVP		Fluorescence	0.114±0.002 µM	0-50 µM	Present work
Sulfur QDs	Tartrazine	Fluorescence	39 nM	0.1-20 µM	[15]
Carbon QDs		Fluorescence	480 nM	0-70 µM	[16]
Carbon QDs		Fluorescence	26 nM	0.1-6 µM	[17]
CdTe-PVP		Fluorescence	0.044±0.001	0-50 µM	Present work

		µM			
CdTe@ZnTe-PVP		Fluorescence	0.042±0.001 µM	0-50 µM	Present work

Table S2: Quenching parameters obtained for the interaction of synthesized CdTe-PVP and CdTe@ZnTe-PVP QDs with HSA at different temperatures (288, 298 and 308 K) in a 20 mM phosphate buffer of pH 7.4.

	Temp. K	K_{SV} **(10^5, M^{-1})**	k_q **(10^{13}, M^{-1} s^{-1})**
HSA-CdTe-PVP	288	0.638±0.017	1.084±0.029
	298	0.631±0.013	1.071±0.023
	308	0.623±0.083	1.056±0.012
HSA-CdTe@ZnTe-PVP	288	1.131±0.068	1.920±0.013
	298	1.062±0.012	1.804±0.021
	308	0.836±0.045	1.419±0.078

Table S3: Calculated distance (*r*) between donor and acceptor molecules in FRET system (CdTe-PVP/CdTe@ZnTe-PVP- food dyes)

FRET system	***r* value (nm)**
CdTe-PVP-carmoisine	5.29
CdTe-PVP-Ponceau 4R	4.79
CdTe-PVP-Tartrazine	4.30
CdTe@ZnTe-PVP-carmoisine	5.57
CdTe@ZnTe-PVP-Ponceau 4R	5.36
CdTe@ZnTe-PVP-Tartrazine	4.77

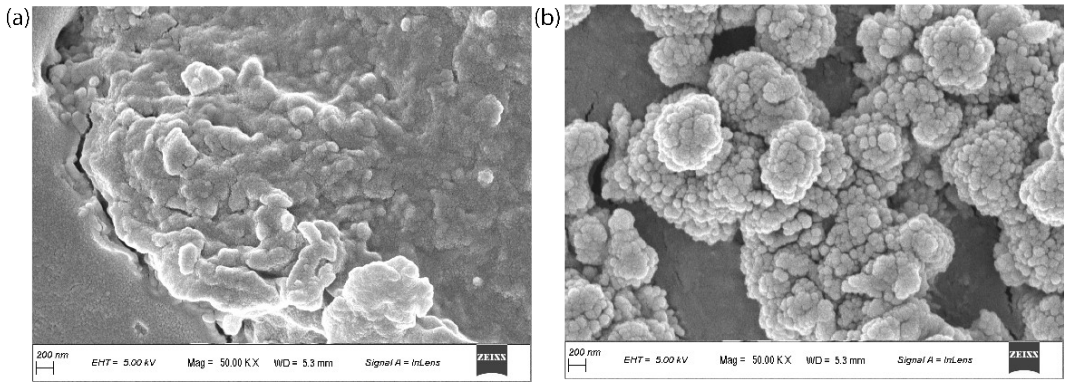

Figure S1. FESEM images of as-synthesized QDs, (a) CdTe-PVP QDs and (b) CdTe@ZnTe-PVP QDs.

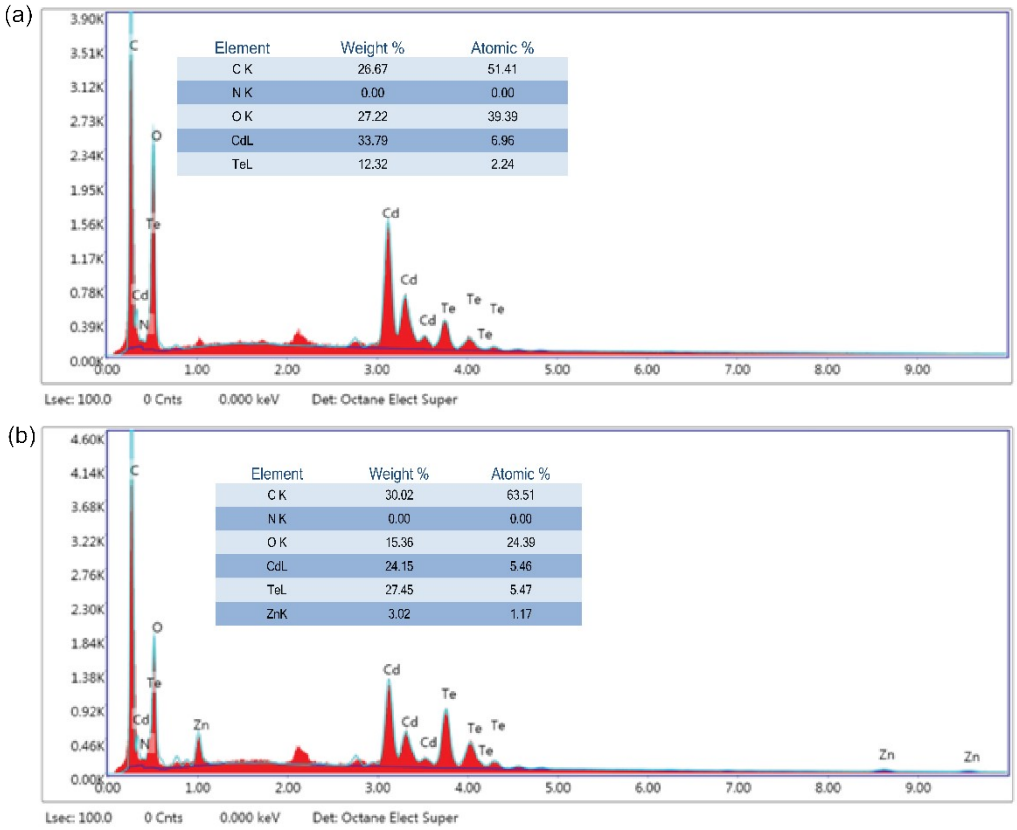

Figure S2. EDX spectra of synthesized QDs, (a) CdTe-PVP and (b) CdTe@ZnTe-PVP QDs.

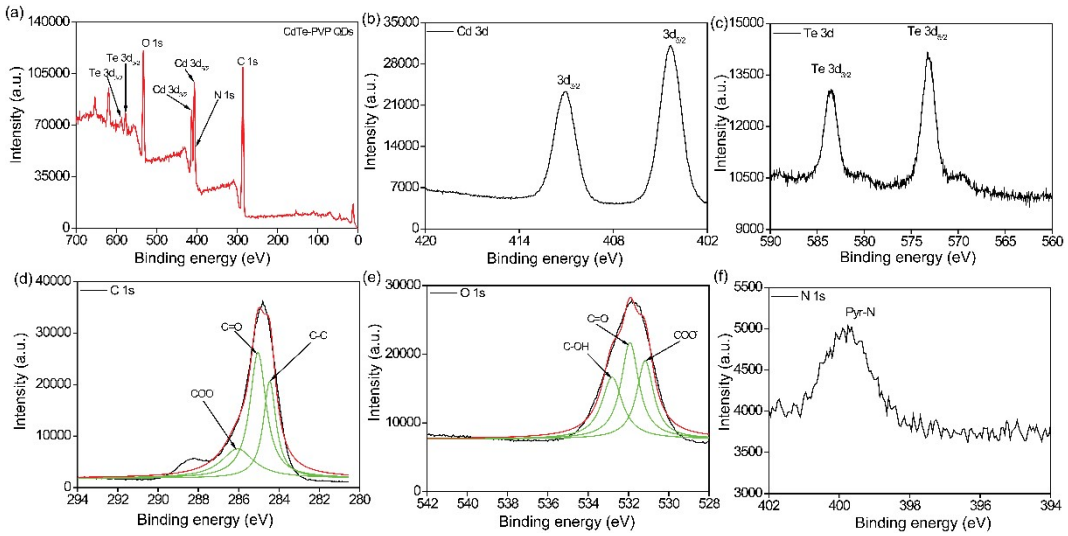

Figure S3. XPS spectra of synthesized CdTe-PVP QDs. (a) survey spectrum, (b) Cd 3d, (c) Te 3d, (d) deconvoluted C 1s spectrum, (e) deconvoluted O 1s spectrum and (f) deconvoluted N 1s spectrum.

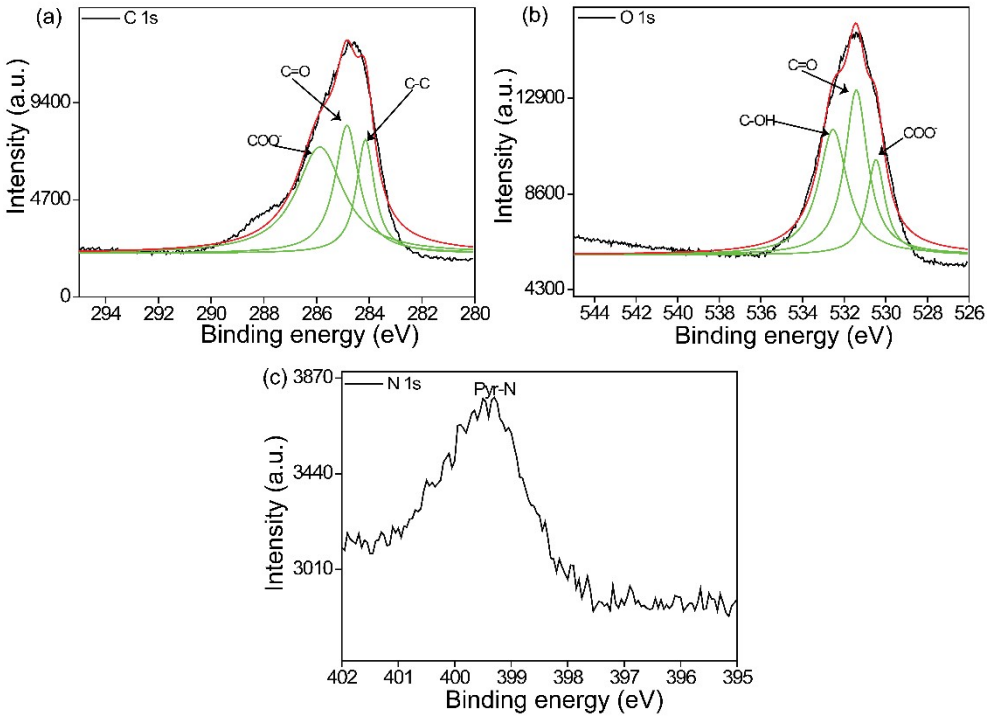

Figure S4. XPS spectra of synthesized CdTe@ZnTe-PVP QDs, (a) deconvoluted C 1s spectrum, (b) deconvoluted O 1s spectrum and (c) deconvoluted N 1s spectrum.

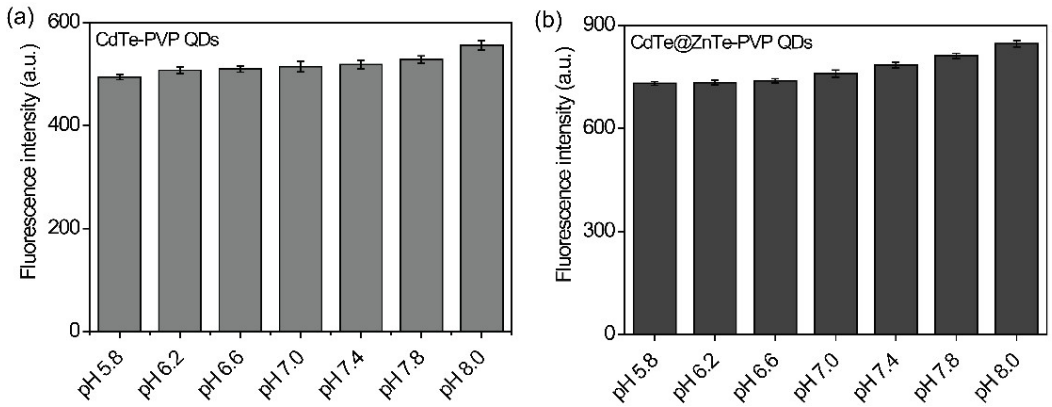

Figure S5. Effects of pH on the fluorescence of CdTe-PVP and CdTe@ZnTe-PVP QDs at different pH (5.8 to 8.0).

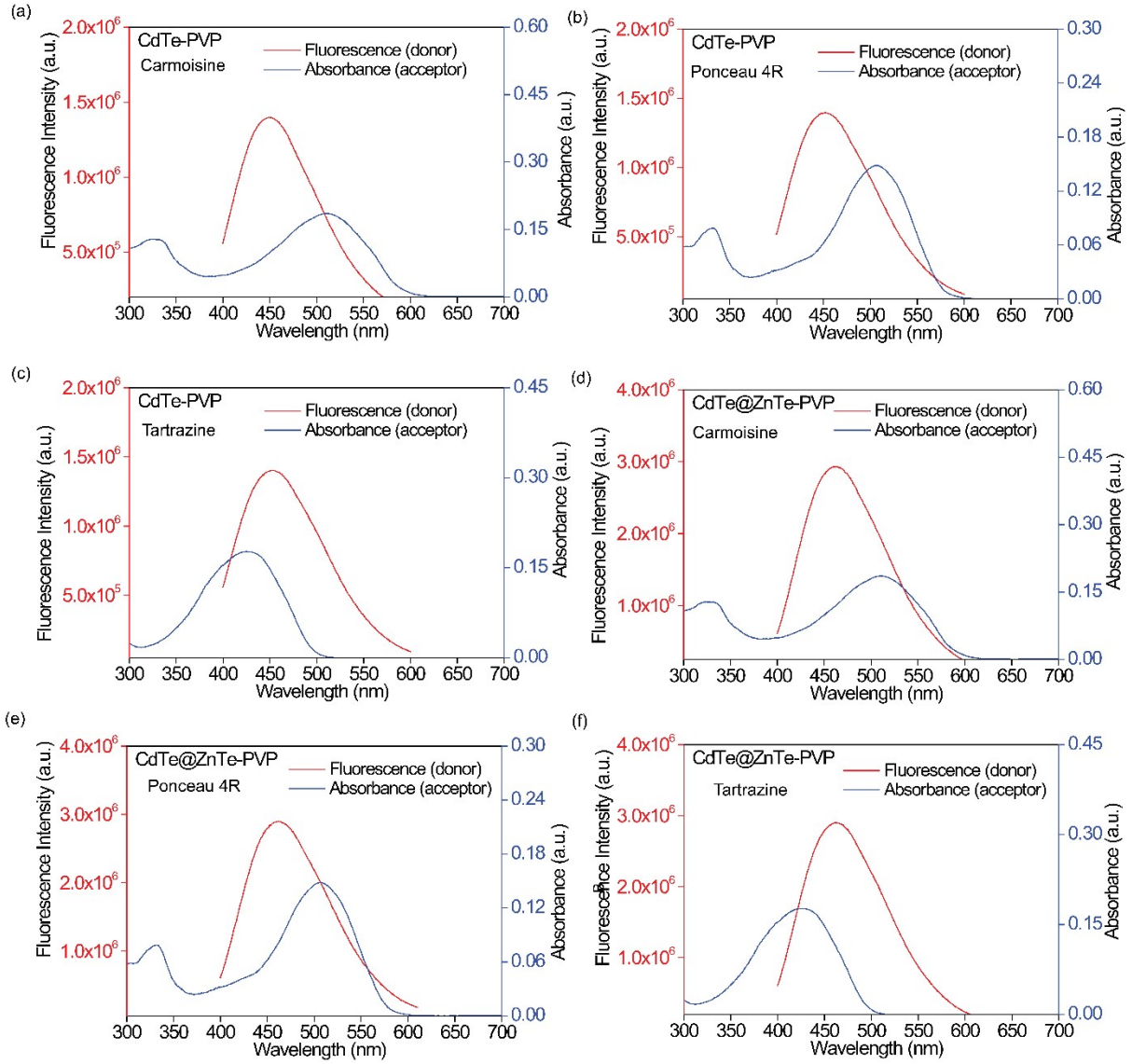

Figure S6. Overlap spectra of donor (QDs)-acceptor (food dye) FRET pair. (a) CdTe-PVP-carmoisine, (b) CdTe-PVP-ponceau 4R, (c) CdTe-PVP-tartrazine, (d) CdTe@ZnTe-PVP-carmoisine, (e) CdTe@ZnTe-PVP-ponceau 4R and (f) CdTe-PVP-tartrazine.

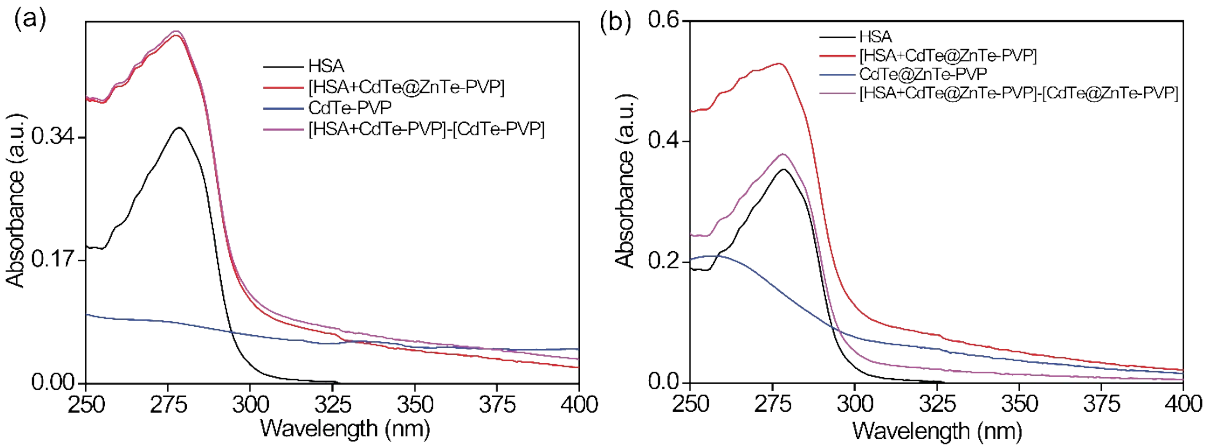

Figure S7. UV-visible spectra of HSA (10 µM) and HSA-QDs (1:1 complex) interactions. (a) HSA and HSA-CdTe-PVP QDs and (b) HSA and HSA-CdTe@ZnTe-PVP QDs in 20 mM phosphate buffer of pH 7.4.

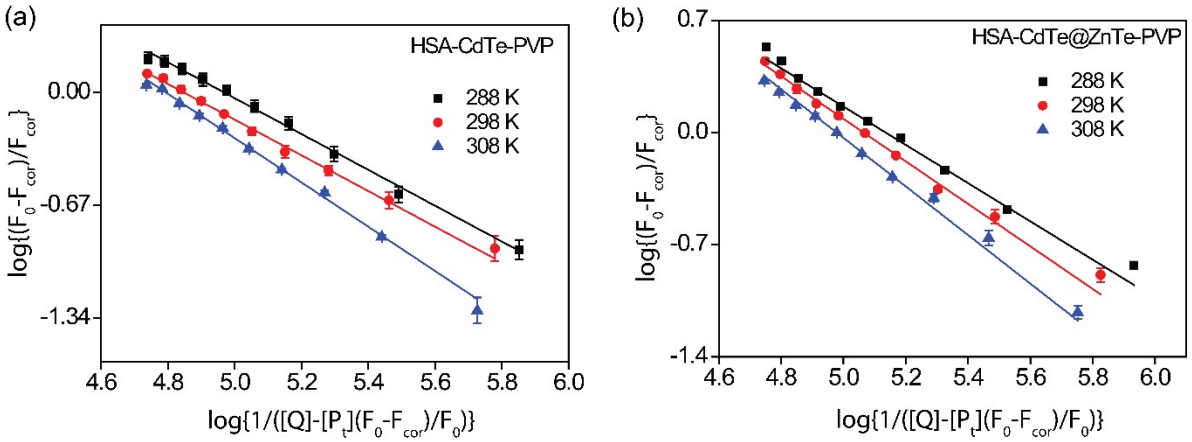

Figure S8. Double logarithm plot of HSA-QDs interactions. (a) CdTe-PVP and (b) CdTe@ZnTe-PVP QDs in a 20 mM phosphate buffer of pH 7.4 at different temperatures (288, 298 and 308 K). [HSA] = 3 μM, [CdTe-PVP] = [CdTe@ZnTe-PVP] = 0-19.7 μM.

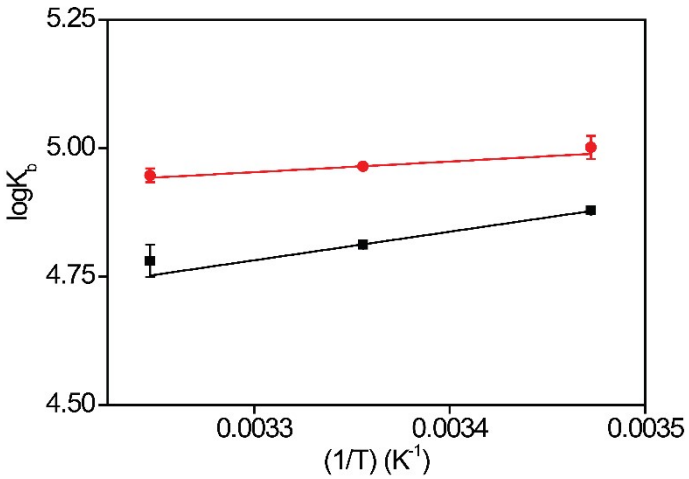

Figure S9. van't Hoff plots for the ineractions of CdTe-PVP and CdTe@ZnTe-PVP QDs with HSA at different temperatures (288, 298 and 308 K) in 20 mM phosphate buffer of pH 7.4.

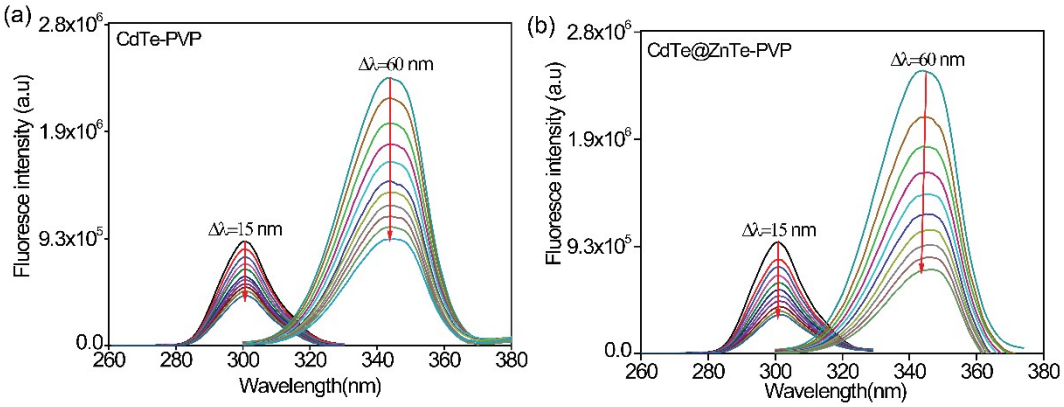

Figure S10. Synchronous emission spectra of HSA (3 μM) in the absence and presence of (a) CdTe-PVP (0-19.7 μM) and CdTe-PVP QDs (0-19.7 μM) at an offset of 60 nm for Trp and 15 nm for Tyr, in 20 mM phosphate buffer of pH 7.4.

2.1. Red edge excitation shift measurements (REES)

REES measurement technique is commonly used to decipher the microenvironment changes around the Trp (Trp 214 for HSA) residue, i.e., motional restriction. REES phenomenon, i.e., the shift of emission maximum toward higher wavelength region upon increase in excitation wavelength, is caused by the electronic interactions between indole moieties of Trp residues with the nearby dipoles at slow solvent relaxation medium.[18] The emission maximum of HSA was observed to be 346 and 350 nm upon excitation at 295 and 305 nm, respectively (**Figure S10**). For the complexes of HSA with the CdTe-PVP and CdTe@ZnTe-PVP QDs, emission maxima were noticed to be 345 and 342 nm, respectively, at an excitation wavelength of 295 nm, whereas 348 and 347 nm were found upon excitation at 305 nm (**Figure S10**). Thus, for native HSA, 4 nm REES effect was indicated, whereas, for the HSA-CdTe-PVP and HSA-CdTe@ZnTe-PVP QDs complexes, reasonable 3 and 5 nm REES effects were found. These findings indicated that there was an effect on the mobility of the Trp 214 residue upon complexation with the respective QDs, i.e., the mobility of the Trp 214 residue was reduced in the presence of respective QDs.

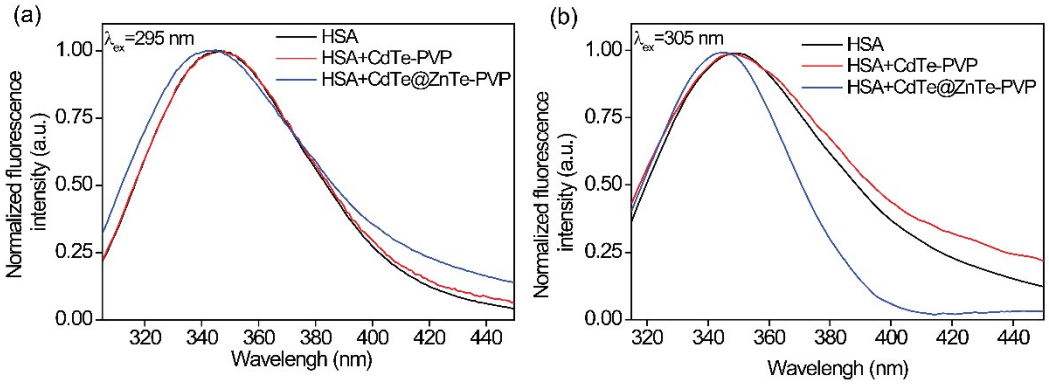

Figure S11. REES effect of HSA and its complexes with synthesized QDs, (a) HSA, HSA-CdTe-PVP and HSA-CdTe@ZnTe-PVP at an excitation wavelength of 295 nm, and (b) HSA, HSA-CdTe-PVP and HSA-CdTe@ZnTe-PVP at an excitation wavelength of 305 nm, in 20 mM phosphate buffer of pH 7.4.

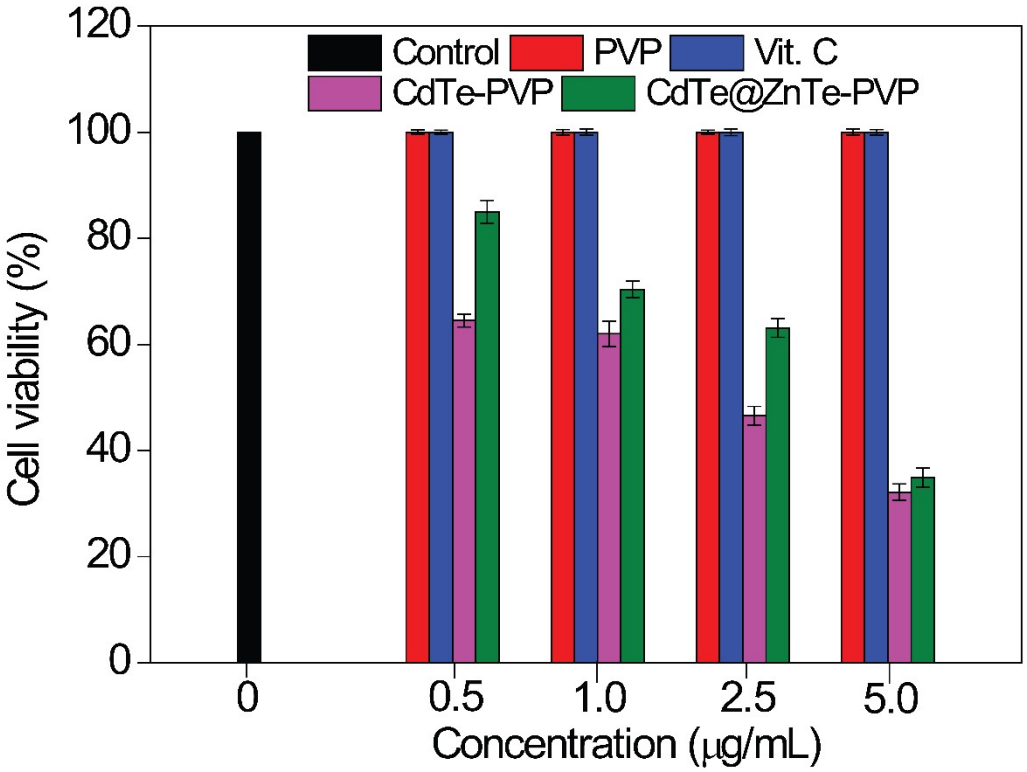

Figure S12. Percentage cell viability of rat skeletal muscle cells (L6) in the absence (control) and presence of PVP, Vit. C, CdTe-PVP and CdTe@ZnTe-PVP QDs at different concentrations (0.5, 1.0, 2.5, and 5 μg/mL).

References

1 M. Haque, S. Lyndem and A. Singha Roy, *Luminescence*, 2022, **37**, 837–853.
2 J. N. Miller, *Proc. Anal. Div. Chem. Soc.*, 1979, **16**, 203–208.
3 D. V. O'Connor and D. Phillips, *Time-Correlated Single Phot. Count.*, 1984, 103–131.
4 L. Whitmore and B. A. Wallace, *Nucleic Acids Res.*, 2004, **32**, W668-73.
5 D. F. Eaton, *J. Photochem. Photobiol. B Biol.*, 1988, **2**, 523–531.
6 W. Zhou, D. T. Schwartz and F. Baneyx, *J. Am. Chem. Soc.*, 2010, **132**, 4731–4738.
7 A. R. Clapp, I. L. Medintz, J. M. Mauro, B. R. Fisher, M. G. Bawendi and H. Mattoussi, *J. Am. Chem. Soc.*, 2004, **126**, 301–310.
8 V. Biju, A. Anas, H. Akita, E. S. Shibu, T. Itoh, H. Harashima and M. Ishikawa, *ACS Nano*, 2012, **6**, 3776–3788.
9 V. Bagalkot, L. Zhang, E. Levy-Nissenbaum, S. Jon, P. W. Kantoff, R. Langery and O. C. Farokhzad, *Nano Lett.*, 2007, **7**, 3065–3070.
10 H. Beitollahi, F. G. Nejad, Z. Dourandish and M. R. Aflatoonian, *Chemosphere*, 2023, **337**, 139369.
11 F. Garkani Nejad, I. Sheikhshoaie and H. Beitollahi, *Food Chem. Toxicol.*, 2022, **162**, 112864.
12 S. Z. Mohammadi, S. Tajik, F. Mousazadeh, E. Baghadam-Narouei and F. Garkani Nejad, *Micromachines*, 2023, **14**, 1433.
13 J. Zhang, L. Na, Y. Jiang, D. Lou and L. Jin, *Anal. Methods*, 2016, **8**, 7242–7246.
14 L. A. Esmail and H. S. Jabbar, *Diam. Relat. Mater.*, 2023, **139**, 110334.
15 X. Peng, Y. Wang, Q. Wang, J. Tang, M. Zhang and X. Yang, *Spectrochim. Acta - Part A Mol. Biomol. Spectrosc.*, 2022, **279**, 121454.
16 L. He and H. Du, *J. Food Compos. Anal.*, 2023, **118**, 105200.
17 S. Thulasi, A. Kathiravan and M. Asha Jhonsi, *ACS Omega*, 2020, **5**, 7025–7031.
18 A. Chattopadhyay and S. Haldar, *Acc. Chem. Res.*, 2014, **47**, 12–19.